Towards 1 kW power production in a reverse electrodialysis pilot plant with saline waters and concentrated brines[☆]

Michele Tedesco[a,b], Andrea Cipollina[a,*], Alessandro Tamburini[a], Giorgio Micale[a]

[a] *Dip. di Ingegneria Chimica, Gestionale, Informatica, Meccanica (DICGIM), Universitá di Palermo (UNIPA) Viale delle Scienze Ed.6, 90128 Palermo, Italy*
[b] *Wetsus, European Centre of Excellence for Sustainable Water Technology, Oostergoweg 9, 8911 MA Leeuwarden, The Netherlands*

Abstract

Reverse Electrodialysis (RED) is a promising technology to extract energy from salinity gradients, especially in the areas where concentrated brine and saline waters are available as feed streams. A first pilot-scale plant was recently built in Trapani (Italy), and tested with real brackish water and brine from saltworks. The present work focuses on the scale-up of the pilot plant, reaching more than 400 m^2 of total membrane area installed and representing the largest operating RED plant so far reported in the literature. With a nominal power capacity of 1 kW, the pilot plant reached almost 700 W of power capacity using artificial brine and brackish water, while a 50% decrease in power output was observed when using real solutions. This reduction was likely due to the presence of non-NaCl ions in relatively large concentration, which negatively affected both the electromotive force and stack resistance. These results provide relevant and unique information for the RED process scale-up, representing the first step for the feasibility assessment of RED technology on large scale.

Keywords: Salinity Gradient Power, RED, REAPower, ion exchange membrane, brine, brackish water.

1. Introduction

Renewable energies are constantly strengthening their position in the energy system worldwide, and exploiting novel energy sources is nowadays a research area of growing interest. Aside to well-established technologies such as solar, wind and hydropower, other renewable energies will play an important role in the near future, thanks to their intrinsically large potential. In this regard, a good example of unexploited energy source is salinity gradient power (SGP), i.e. the energy available by mixing in a controlled way two solutions with different salt concentration, for example river water and seawater [1–4]. The amount of energy theoretically available from salinity gradients is remarkably high, with an estimated power in the range of 1.4–2.6 TW based on the global discharges of rivers into oceans [5], without considering several alternative applications of SGP, such as closed-loop storage

[☆]**Please cite this article as:** M. Tedesco, A. Cipollina, A. Tamburini, G. Micale, *Towards 1 kW power production in a reverse electrodialysis pilot plant with saline waters and concentrated brine*, Journal of Membrane Science, 522 (2017) 226-236

[*] *Corresponding Author:* andrea.cipollina@unipa.it (A. Cipollina)

and conversion of energy or SGP coupling with desalination [6]. The conversion of such energy source into mechanical/electrical power can be accomplished by a number of processes, namely: pressure-retarded osmosis (PRO) [7], reverse electrodialysis (RED) [8], the class of accumulator-mediated mixing processes (AccMix) [9] (among which the capacitive mixing based on double-layer expansion (CDLE) [10], and the membrane-modified supercapacitor flow cell [11]), and a recent process based on hydrogels swelling [12]. All of these processes have reached nowadays different levels of technological maturity, ranging from proof-of-the-concept to laboratory demonstration and pilot systems. In this regard, reverse electrodialysis (RED) represents one of the most investigated SGP technologies, and currently the only one - together with PRO - already tested on pilot scale [13, 14].

The principle of RED process operation is based on the conversion of salinity difference into electric current, thanks to the selective properties of ion exchange membranes (IEMs) [15]. A RED device (or stack) consists of an alternating series of cation and anion exchange membranes (CEMs, AEMs), separated by spacers to create channels. During the process operation, the system is fed with a concentrate and a dilute solution, e.g. seawater ($\sim$30 g/l NaCl) and river water ($\sim$1 g/l NaCl). The ion flux from concentrate to dilute channels is regulated by the permselectivity of membranes, allowing - ideally - only cations to pass through CEMs, and only anions to pass through AEMs. As a result, an ionic current is generated through the stack, then converted into electric current by means of electrode reactions, and can be eventually collected by an external electrical load.

The RED process has been widely assessed as a viable technology under different conditions, especially for the case of NaCl solutions. A growing literature is dedicated to the influence of some major parameters on the process performance, such as: membrane structure [16–19], spacer geometry [20, 21], feed concentration [22–25], flow rates [26], and temperature [27, 28]. Current efforts are focused on the development of membranes with higher selectivity towards monovalent ions [16], and on spacer-less design by using profiled membranes, which have been shown experimentally to be able to increase the net power density compared to systems with spacer-filled channels [29]. Feed conditions have also a notable impact on RED performance: for instance, if river water is used as dilute solution, $\sim$45% of the ohmic losses in the system are caused by the dilute channels [30]. In this regard, blending the dilute and the concentrated feeds before the stack entrance has been proposed as a strategy to enhance the system power output, by decreasing the stack resistance [31]. Another option for reducing the internal resistance is the use of more concentrated solutions, such as saline waters and brines: in particular, laboratory tests performed with artificial brackish water (0.1 M NaCl) and brine (5 M NaCl) have demonstrated the possibility to reach a power density up to 12 W/m^2 of cell pair [23]. Moreover, a recent critical review on pressure-retarded osmosis (PRO) by Straub et al. confirmed that the use of hypersaline solutions might be a promising option for energy harvesting from salinity gradients, and identifying new sources for concentrated streams is therefore crucial [32].

Despite the notable improvements reached on the laboratory scale, further research is still needed to address the feasibility of the process up-scaling, and make the RED technology economically attractive. In fact, very limited experimental information has been reported so far on the performance

of the RED process using natural feed steams. In 2014, the first RED demonstration plant operated with real concentrated brines and saline waters has been built in Trapani (Italy), as a main goal of the REAPower project [33]. In this pilot installation, a RED stack with 125 cell pairs of 44x44 cm^2 membrane area (i.e. $\sim$50 m^2 of IEMs installed) was tested with real brackish water and saturated brine from saltworks, producing an average gross power around 40 W ($\sim$1.6 W/m^2 cell pair), with peak values up to 60 W ($\sim$2.6 W/m^2 cell pair) [14].

In this work, we present the scale-up of the above-mentioned pilot plant, carried out through the additional installation of two larger RED units, each one equipped with 500 cell pairs with a 44x44 cm^2 membrane area. In its final configuration, the pilot plant consists of 3 RED units with $\sim$400 m^2 of total membrane area installed, thus representing the largest RED installation so far reported in the literature. The RED units were tested both with real solutions (brackish water and brine) and with artificial NaCl solutions, under similar operating conditions. The results reported show the feasibility of the RED process on larger scale, providing an important step towards the technology industrialization.

2. Plant construction and commissioning

2.1. The REAPower pilot plant: from the concept idea to the first operating prototype

The design, construction, installation and testing of the REAPower pilot plant has been the outcome of a 4-year European research project (2010-2014) [33]. During the 4-year lifetime of the REAPower project, research activities have been focused on several aspects related to the use of concentrated solutions in the system, as well as the environmental constraints given by the plant location. The use of concentrated solutions as feed streams cause significant differences in the membrane behaviour, thus novel ion exchange membranes were developed to have better performance in high salt concentration range. The following sections summarise the main steps that have eventually led to the installation of the RED pilot plant.

2.1.1. The concept idea: reverse electrodialysis from saline waters and concentrated brine

The idea of using concentrated brines and saline waters to generate the salinity gradient was at the origin of the project, based on the following considerations: i) large salinity gradient and, thus, energy density could be achieved; ii) optimal operating conditions could be easily identified in order to reduce the overall stack resistance (i.e. by using a saline water as LOW feed solution), and maximise the obtained power density; iii) the salinity gradient can be naturally restored if the exhausted HIGH feed solution is re-circulated to saltworks basins, where sun and wind cause the evaporation of water, thus concentrating again the solution. Laboratory investigation and process modelling activities have supported the design of the system and helped in preliminarily identifying the potentials and weaknesses of the concept idea [23, 34].

2.1.2. Lab-scale investigation of optimal operating conditions

In order to characterise the RED process behaviour in such "non-conventional" operating conditions and to identify optimal operating ranges, two RED units with different size were tested at the

laboratory scale [23]: a small one, with 50 cell pairs of 10x10 cm^2 membrane area, and a large one, with 100 cell pairs of 20x20 cm^2 membrane area. Results demonstrated how the increase in flow velocity can slightly enhance the gross power output, though values above a critical velocity (2–3 cm/s for the investigated units and conditions) lead to unacceptable hydraulic losses, even resulting into a negative net power output [23]. Moreover, the increase in the HIGH feed solution concentration lead to significant benefits in terms of salinity gradient, electromotive force and power output, though very high concentration can lead to a significant reduction in the IEMs permselectivity, thus negatively affecting the actual process yield.

The dilute feed solution concentration (C_{LOW}) can play a major role in the process performance optimisation. In fact, maximum power output was achieved with C_{LOW} ranging between 0.01 M and 0.1 M NaCl. This large optimal range results from the counteracting effects that the dilute concentration has on the process operations. In particular, lower values of C_{LOW} tend to: i) increase the overall stack resistance; ii) enhance the salinity gradient (i.e. the electromotive force of the RED pile). These two counteracting effects can have a stronger/weaker influence depending on the stack geometry and process operations. For instance, reducing the channel thickness or increasing the salt concentration of the dilute (e.g. by partial blending with the concentrate) has the advantage of decreasing the dilute compartment resistance [31]. On the other side, thicker channels make the influence of C_{LOW} on the stack resistance more important, while long residence times make the average concentration in the LOW compartment much larger than the inlet one, thus reducing the effect of C_{LOW} on the overall process performance. Therefore, the best value of C_{LOW} has to be identified case by case for system optimisation.

2.1.3. Computational Fluid Dynamic modelling and process simulation

A multi-scale process simulator for the RED process with concentrated solutions was developed [34, 35], in order to describe the effect of high salt concentrations on solutions properties (e.g., electrical conductivity and activity coefficients), and analyse the behaviour of the system. The multi-scale approach was based on the use of Computational Fluid Dynamic (CFD) tools for the characterisation of system behaviour at the micro-scale, focusing on fundamental phenomena such as concentration polarisation, and pressure drops inside the compartments and in the inlet/outlet manifolds [21, 36]. Then, a process simulator with a hierarchical structure was developed, which also included the main findings of CFD simulations at the micro-scale [34]. This allowed us to identify optimal conditions for the pre-pilot system and support the design the pilot plant, simulating the operation of the plant using brackish water and brine as feed streams in the final pilot-scale.

2.1.4. Installation and testing of the first RED prototype

The final goal of the REAPower project has been the installation of a RED demonstration plant operating with brackish water and brine in a real environment [37]. The plant is located in a saltworks area in Marsala (Trapani, South of Italy): this location provides brackish water from a shoreline well and concentrated brine from saltworks as feed solutions. A first RED unit (designed and built by the project partner REDstack B.V.) with 44x44 cm^2 membrane area and 125 cell pairs was initially

installed and tested for five months [14]. During this first experimental campaign, a power output of 63 W (2.6 W/m^2 cell pair) was achieved using artificial solutions, while testing the RED unit under similar conditions with real brackish water and brine, a ∼50% decrease of the performance was observed. This was mainly attributed to the presence of other ions (especially Mg^{2+}), which are present in relevant amount in the brine.

Bivalent ions negatively affect membranes properties, causing a reduction of permselectivity (up to 50% compared to NaCl [38]), and a significant increase of the electrical resistance. Moreover, uphill transport of Mg^{2+} and SO_4^{2-} has been observed in RED process with seawater–fresh water conditions, thus causing a further decrease of the available OCV [39, 40]. For these reasons, the removal of Mg^{2+} from feed waters might be required during the pre-treatment stage of RED plants. This could be done synergically with $Mg(OH)_2$ recovery from the brine, thus obtaining also a valuable by-product of the process [41, 42]. Alternatively, the use of mono-selective membranes or IEMs with low-resistance to the passage of bivalent ions might represent a valuable strategy, though recent studies have shown that the development of high-performance membranes to increase power density is still challenging [16].

Interestingly, no drops in plant performance were observed in the long period of operation of the pilot system, indicating that RED technology with brine and brackish water as feed solutions does actually present a good robustness and suitability for continuous operation in a real environment.

2.2. Plant scale-up and operational procedures

In addition to the first prototype described in [14], two larger RED units with 500 cell pairs of 44x44 cm^2 membrane active area were installed in the plant. Slight modifications to the plant layout and auxiliary units were implemented during the plant scale-up, thus only a short description of the pilot plant is reported here, while more information can be found in [14].

A simplified scheme of the final plant layout is shown in Fig. 1. From the two intakes (concentrated brine basins and brackish water well), the feed water is pumped to a filtering unit (a washable filter of 50 μm mesh, plus 2 PP filters with 20 and 5 μm mesh), and then stored in two 125 litres buffering tanks. From these reservoirs, two controllable-speed magnetic-drive centrifugal pumps (Schmitt MPN 130, Kreiselpumpen GmbH & Co. KG, Germany) are used to circulate the feed solutions to the three units. A hydraulic distribution system is used to feed each single RED unit at one time or to feed in parallel 2 or 3 of them. Flow, pressure, conductivity and temperature measuring devices allow to monitor the feed solutions flow rate and properties.

The electrode rinse solution consists of an aqueous solution with 0.3 M $FeCl_2$, 0.3 M $FeCl_3$, and 2.5 M NaCl as supporting electrolyte. A small amount of HCl was dosed to keep the pH around 2-3, in order to avoid precipitation of iron compounds [43]. The electrode rinse solution was circulated by a controllable-speed magnetic-drive centrifugal pump (Schmitt MPN 130, Kreiselpumpen GmbH & Co. KG, Germany), which was connected to a distribution circuit to feed alternatively each single RED unit or in parallel 2 or 3 of them. Thanks to a separate hydraulic circuit with two 2 m^3 tanks, the plant was also operated using artificial NaCl solutions. The small prototype is placed on a main supporting

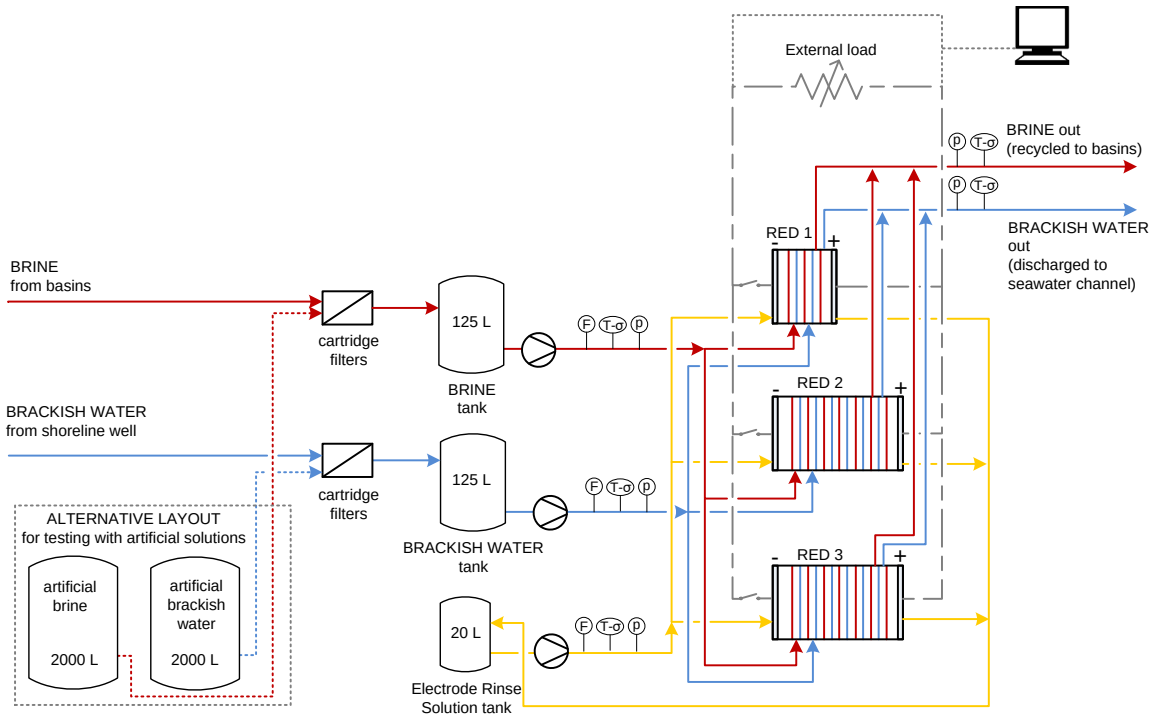

Figure 1: Simplified scheme of the plant layout. The 3 RED modules can be operated in parallel both hydraulically and electrically (with a common variable external load).

tray (Fig. 2.A), together with buffer tanks and auxiliary equipment, while the large prototypes are installed in the same room (Fig. 2.B), but positioned on different supporting trays. Geometrical details of the 3 RED prototypes are reported in Tab. 1. Each RED unit is equipped with ion exchange membranes purposely developed for highly concentrated solutions (Fujifilm Manufacturing Europe BV, The Netherlands). The main properties of such membranes are listed in Tab. 2.

Table 1: RED units installed in the REAPower pilot plant in Marsala (Trapani, Italy).

RED unit	Membrane area (cm^2)	Cell pairs	Total cell pair area (m^2)	Stack dimensions (ca) (m x m x m)
STACK-1	44 x 44	125	24	0.8 x 0.8 x 0.3
STACK-2	44 x 44	500	97	0.8 x 0.8 x 0.8
STACK-3	44 x 44	500	97	0.8 x 0.8 x 0.8

After the installation of the two large prototypes, the construction of a new electric circuit was necessary to fit the new range of required external resistance. In fact, the larger stacks have a lower stack resistance than the small prototype. Ten halogen lamps were installed according to the electrical scheme shown in Fig. 3. Each lamp has a nominal power of 100 W at a standard voltage of 24 V (actual possible operating range: 6–30 V), thus providing an electric resistance of ~5.8

Table 2: Properties of ion exchange membranes installed in the REAPower pilot plant*.

Membrane	Thickness (μm)	Permselectivity[a] (-)	Electrical resistance[b] (Ω cm^2)	Hydraulic permeability (mL/bar h m^2)	Ion Exchange Capacity (meq/g)
AEM RP1 80045-01	120	0.65	1.55	4.96	1.28
CEM RP1 80050-04	120	0.90	2.96	4.72	1.45

* Data provided by the manufacturer (Fujifilm Manufacturing Europe BV, The Netherlands).

[a] Permselectivity measured between 0.5 M NaCl–4 M NaCl conditions at 25°C.

[b] Electrical resistance measured in 0.5 M NaCl solution at 25°C.

Ω (the actual resistance can change if a different voltage is applied, in fact the resistance depends on the temperature of the incandescent wire, which varies with the applied voltage and circulating current). Using switches to open/close the parallel branches of the circuit, these lamps were used as variable-resistance load, able to operate at total peak voltage of 50–60 V. During some tests, the two large stacks were electrically connected in parallel, in order to double the total power output without affecting the total voltage (which would result into higher risks for plant operators).

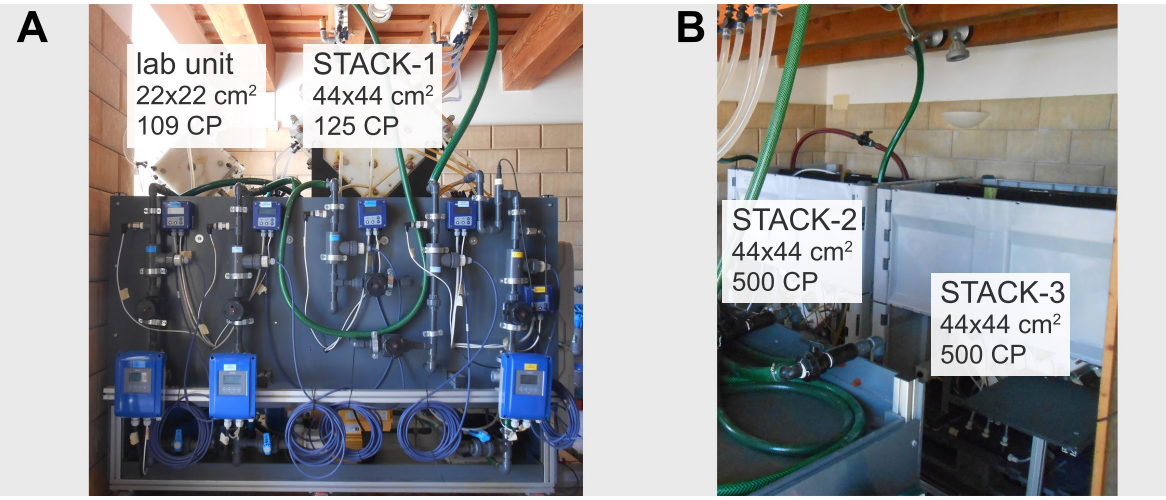

Figure 2: Pictures of the pilot plant. A) Main supporting tray with instrumentation. Two RED units are shown on the tray for visual comparison: a laboratory stack (22x22 cm^2, 109 cell pairs) and the small RED prototype unit (STACK-1), with 44x44 cm^2 125 cell pairs. B) Large RED prototype units (STACK-2, STACK-3), with 44x44 cm^2 500 cell pairs.

2.2.1. Operational procedure

The pilot plant has been operated with natural (real) feed streams, as well as with artificial solutions, in order to highlight the differences caused by varying feed composition. The testing procedure consists of stabilising the hydraulic behaviour of the units, and then performing the power output measurements under variable load conditions, by changing the external resistance in the entire voltage-current (E-I) curve. From the E-I curve, the stack resistance, electromotive force and power

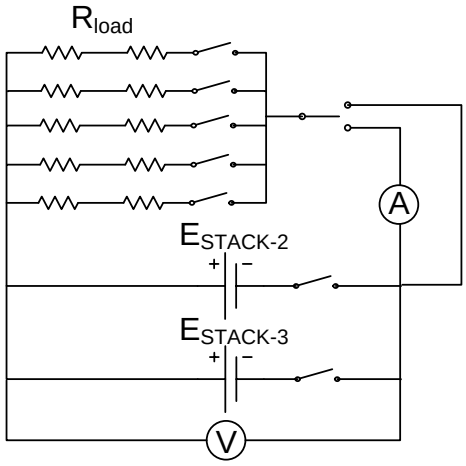

Figure 3: Schematic representation of the external circuit used for power measurements with the large modules (STACK-2, STACK-3); 10 halogen lamps (100 W of nominal power at 24 V), in 5 parallel branches, were used as external load. The equivalent resistance of the circuit under maximum power conditions is in the range of 2–3 Ω.

output can be obtained [14]. Moreover, the measured pressure drops were used to calculate the pumping losses within the units, thus evaluating the net power output of the plant.

Since natural waters can undergo some variations in their composition and NaCl content, and no analytical instruments are available at the test site for online monitoring of feed compositions, the conductivity of feed streams has been selected as a reference variable. Therefore, solution conductivity has been also adopted as a reference for the preparation of artificial solutions, using 99.5% pure NaCl (SOSALT SpA, Italy). For the sake of brevity, further details on experimental procedures and equations to calculate the derived variables are not reported here and can be found in [14].

3. Results and discussion

3.1. Testing with artificial solutions

Following the procedure adopted for the small prototype [14], both large stacks were firstly tested using artificial solutions. In particular, different conditions of inlet conductivity and flow rates were investigated for the dilute feed stream, which mainly affect the system performance [13, 23]. As an example, Fig. 4 shows the effect of dilute (LOW) conductivity on the performance of both large prototypes, in terms of stack voltage and resistance, power output and power density.

The higher inlet concentration of dilute water leads in all cases to a reduction in the OCV. On the other hand, reducing feed conductivity to 0.7 mS/cm, though allowing a higher OCV, leads to an increase in the stack resistance, thus resulting in an overall reduction in the power output. This result is more evident for the STACK-2, which also shows a significant deviation from the linearity in the E-I plot at high current densities (Fig. 4.A). This change in the slope of the E–I plot can be caused by a number of factors that affect the internal resistance, such as non-homogeneous flow distribution in the

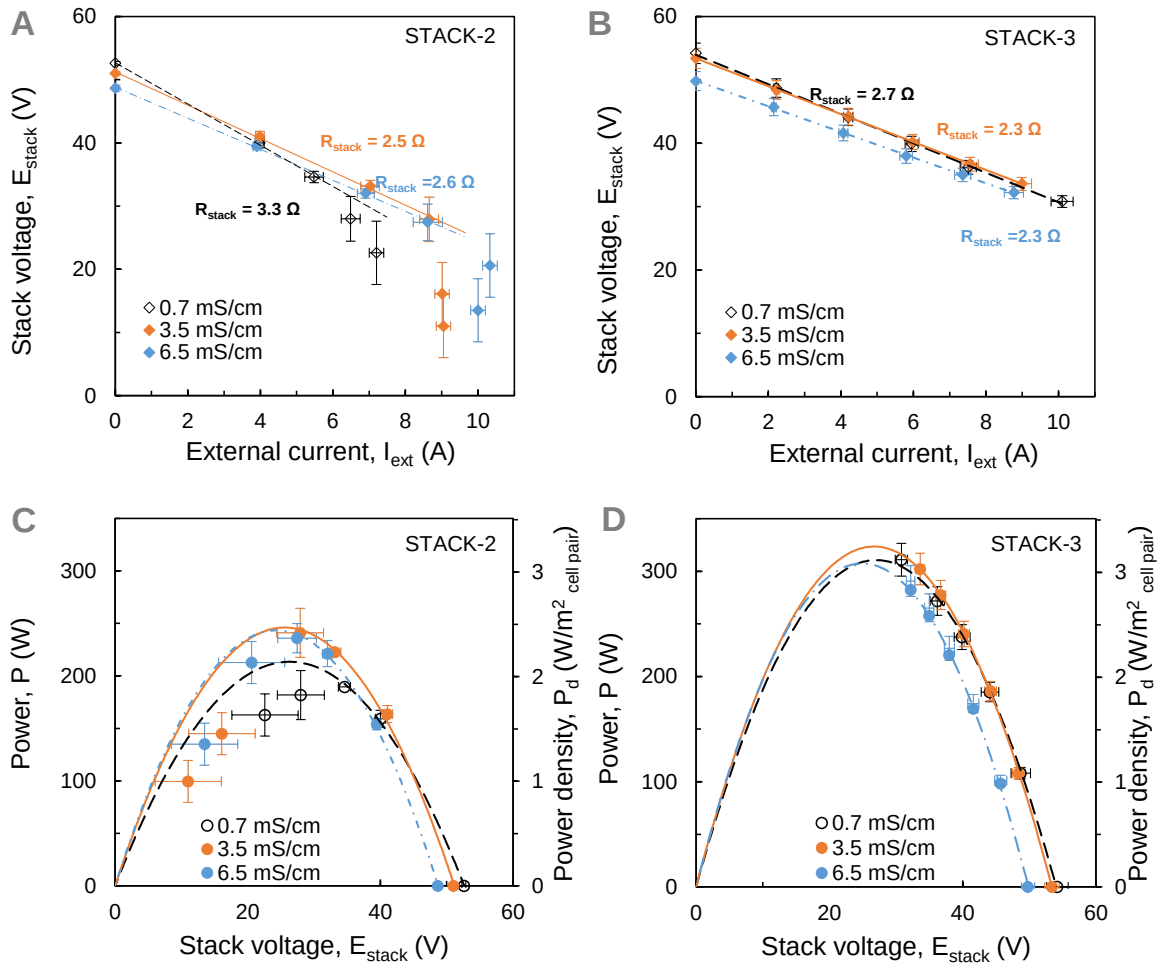

Figure 4: Influence of dilute (LOW) conductivity on process performance. Power measurements performed with large prototypes fed with artificial brine (215 mS/cm) and artificial brackish water. A) Polarization curve for STACK-2. B) Polarization curve for STACK-3. C) Power output curve for STACK-2. D) Power output curve for STACK-3. Concentrate (HIGH) flow rate: 26 l/min (∼0.9 cm/s). Dilute (LOW) flow rate: 34 l/min (∼1.2 cm/s).

compartments (enhancing polarization phenomena), defects in the channels configuration, or limiting current conditions in the electrode compartments [30]. Therefore, the experimental values measured at high current were not considered for the fitting. It is worth noting that such phenomenon is not evident in STACK-3, which showed in all the cases better performance than STACK-2. Although the two units are, in principle, identical, some non-detected differences in stack manufacturing could have caused such diverse behaviour. In particular, this difference might be attributed to improvement in stack making, thus enhancing flow distribution and reducing the internal resistance in STACK-3. However, it was not possible to detect with certainty a possible explanation for this difference of performance between the stacks. The performance of the system does not change appreciably in the range of 3–6 mS/cm of dilute conductivity (i.e. 0.03–0.06 M NaCl). In this case, a power output of more than 320 W (3.3 W/m^2 cell pair) was reached, which is, to the authors' knowledge, the highest value ever achieved with a single RED unit.

Figs. 5–6 report the combined effect of variation in flow rate and concentration of the LOW feed solution for the two stacks. Aside from the experimental scattering of data, it is evident how a lower

feed conductivity leads to an enhancement of both OCV and stack resistance (Fig. 5), counteracting in the final power output (Fig. 6). On the other hand, the effect of flow rate is appreciable only at the lowest flow rate, where the generated power is reduced by 20–30% compared to the maximum values achieved. Also in this case, the difference between stacks is evident in the lower stack resistance and higher OCV and power output of STACK-3.

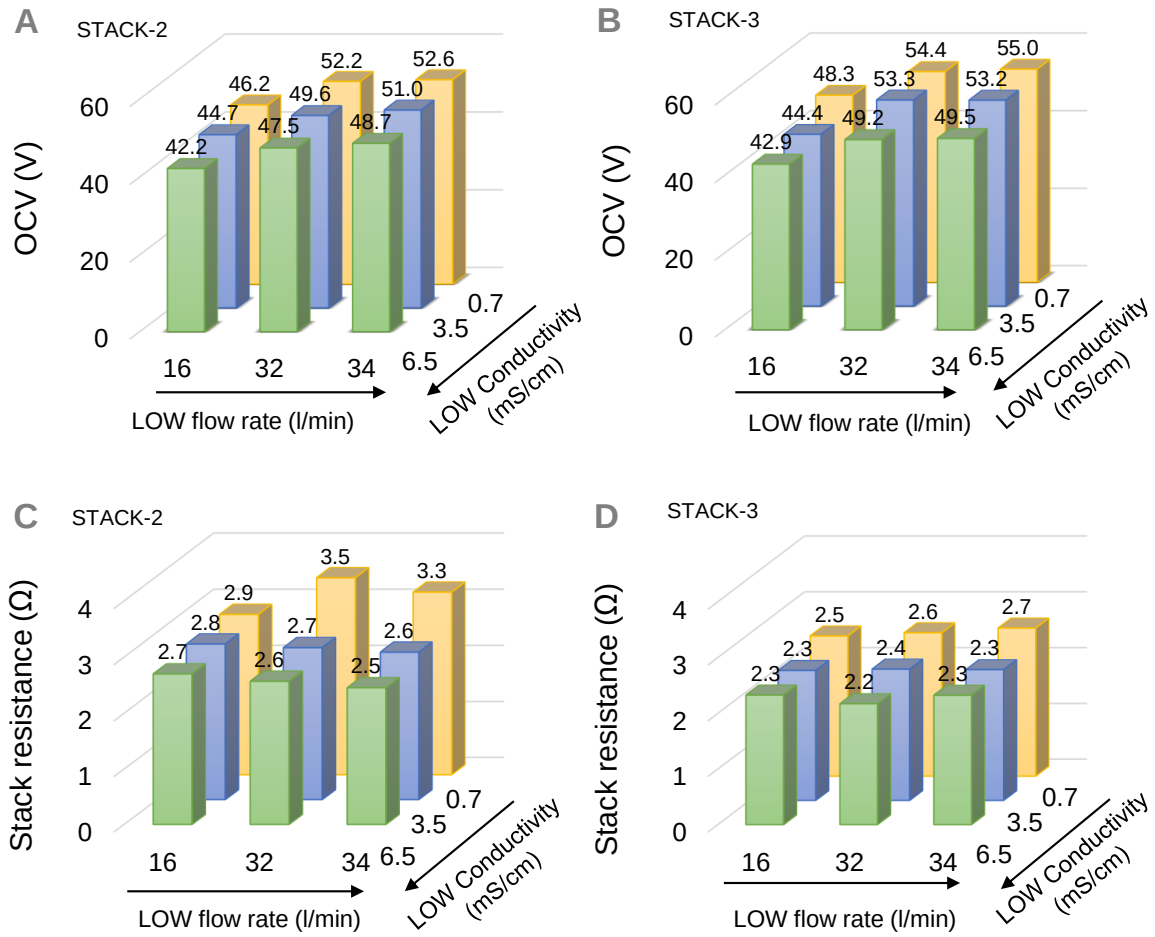

Figure 5: Influence of dilute (LOW) conductivity and flow rate on OCV and stack resistance. A) OCV in STACK-2. B) OCV in STACK-3. C) Stack resistance in STACK-2. D) Stack resistance in STACK-3. Power measurements performed feeding the prototype with artificial brine (NaCl solution at 215 mS/cm, flow velocity ∼0.9 cm/s, T_{HIGH} ∼25 °C) and artificial brackish water (NaCl solution at 0.7–6.5 mS/cm, T_{LOW} ∼25 °C).

3.2. Testing with real solutions

The pilot plant has been operated also using real brine with a conductivity ranging between 190 and 215 mS/cm and brackish water from a shoreline well with a conductivity of 3.4 mS/cm (details on feed solutions composition are reported in Tab. 3). Some additional tests were also carried out feeding the dilute compartments with tap water at 0.7 mS/cm, instead of real brackish water, in order to highlight the effect in changing the LOW concentration also when using real brine.

A summary of tests performed operating the stacks singularly with real solutions is reported in Tab. 4, while Fig. 7 shows a comparison between the performance of the two stacks operated with

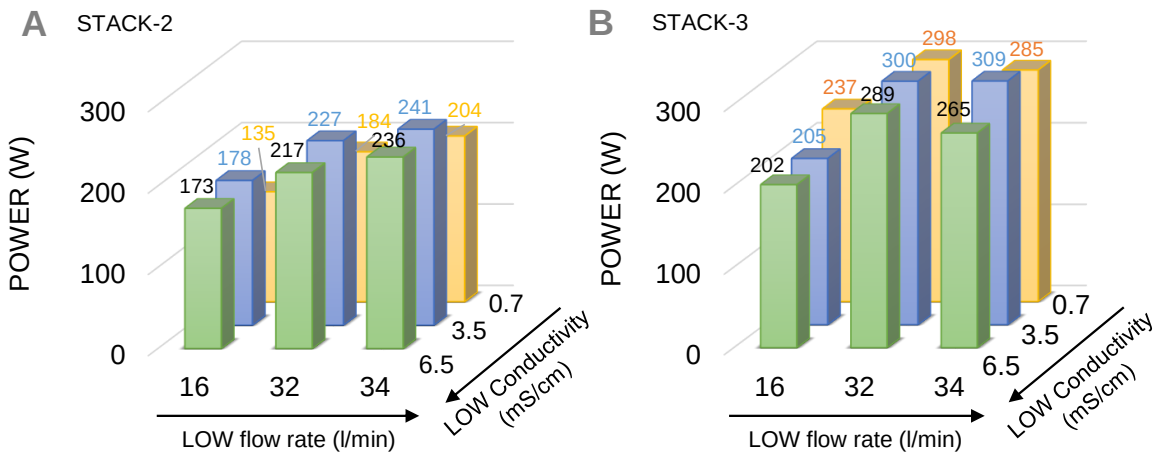

Figure 6: Influence of dilute conductivity and flow rate on power output. A) STACK-2. B) STACK-3. Power measurements performed feeding the prototype with artificial brine (NaCl solution at 215 mS/cm, flow velocity ~0.9 cm/s, T_{HIGH} ~25 °C) and artificial brackish water (NaCl solution at 0.7–6.5 mS/cm, T_{LOW} ~25°C).

Table 3: Characteristics of natural brackish water and brine feed solutions in the saltworks of Ettore e Infersa (Marsala, TP, Italy) [14].

Solution	Conductivity (mS/cm)	T (°C)	Typical ion composition (g/l) [b]					
			Na^+	K^+	Ca^{2+}	Mg^{2+}	Cl^-	SO_4^{2-}
Brine	150–220 [a]	27 (18–31)	64 (48–94)	11 (7–14)	0.4 (0–1.3)	45 (24–58)	192 (175–219)	39 (0–75)
Brackish water	3.4	24 (17–27)	0.41	0.02	0.27	0.08	1.19	0.11

[a] The brine conductivity changes appreciably during seasons, ranging from 150 mS/cm in winter up to 220 mS/cm in summer.

[b] Brine composition can significantly change along the year: the most representative value of concentration is reported for each species, while the typical range of variation is indicated between brackets.

brackish and tap water as the LOW feed solution, and operated with artificial solutions (215 mS/cm and 3.5 mS/cm).

Also with real solutions, STACK-3 showed better performance than STACK-2 in all measurements. The different performance is related to the stack resistance, higher for STACK-2 than for STACK-3, and to the OCV, higher for STACK-3 than for STACK-2. Moreover, in the high-current range, a deviation of the polarisation curve from the linear behaviour was observed for STACK-2, further indicating a lower performance of the unit at high current density values [30] (Fig. 7.A). When using real brine as concentrate and tap water (0.7 mS/cm) as dilute, the lower conductivity of the LOW feed leads to higher OCV values, while slightly increasing the stack resistance, thus resulting in a slightly higher power output obtained for the brine-tap water case.

STACK-2 and STACK-3 were also operated in a parallel arrangement for feed solutions, and

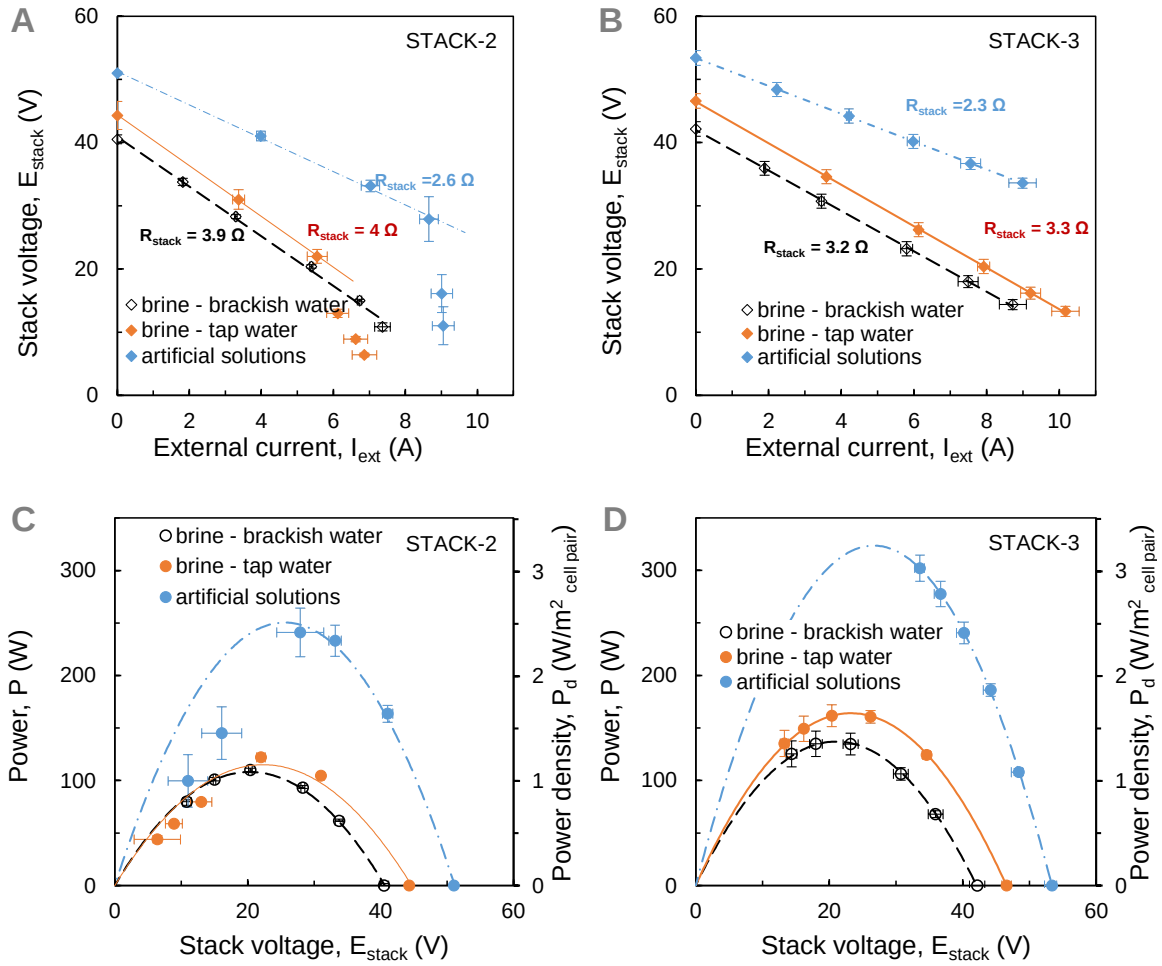

Figure 7: Power measurements performed with real and artificial solutions. A) Polarization curve for STACK-2. B) Polarization curve for STACK-3. C) Power output for STACK-2. D) Power output for STACK-2. Natural brine conditions: conductivity 2105 mS/cm, flow rate ∼26 l/min, T ∼30°C. Natural brackish water conditions: conductivity 3.4 mS/cm (0.7 mS/cm for tap water), flow rate ∼32 l/min, T ∼25°C. Artificial brine conditions: conductivity 215 mS/cm, flow rate ∼26 l/min, T ∼25°C. Artificial dilute conditions: 3.5 mS/cm, flow rate ∼32 l/min, T ∼25°C.

electrically connected in parallel. In these conditions, a stack resistance of 3.4 Ω and 2.8 Ω was measured for STACK-2 and STACK-3, respectively (Fig. 8.A), while the same OCV (forcedly the same, due to the parallel electrical connection) of about 39 V was measured. The maximum power output obtained with real brine and brackish water was ∼230 W (1.4 W/m^2 cell pair), i.e. given by the sum of power obtained in the two single stacks.

It is worth noting that the two large units were fed in parallel with lower flow rates than standard conditions (i.e., 1 cm/s of fluid velocity in single channels [23]). In particular, a total flow rate of $Q_{HIGH} \sim 26$ l/min and $Q_{LOW} \sim 38$ l/min were used, corresponding to single stack fluid velocity in the range of 0.5–0.7 cm/s. This low range of flow velocities causes a slight decline in performance, with respect to the test performed in standard conditions feeding singularly the two stacks. On the other hand, tests with larger flow rates were not possible due to physical limitations in the installed feed pumps. Nevertheless, the power output of the two stacks in parallel is very close to the sum of the power measured for stacks in standard conditions with real solutions, thus allowing to assume

Table 4: Summary of the main results achieved with the larger RED units operated with real solutions. HIGH conductivity: 193-215 mS/cm; HIGH flow rate: ∼ 26 l/min (∼0.9 cm/s); T: 25-30°C.

			STACK-2			STACK-3		
Feed solutions	LOW flow rate (l/min)	LOW conductivity (mS/cm)	OCV (V)	P (W)	Pd (W/m^2)	OCV (V)	P (W)	Pd (W/m^2)
brine/	36	3.4	41.7	123	1.3	44.1	163	1.7
brackish water	32	3.4	41.0	112	1.2	43.4	148	1.5
	16	3.4	38.9	125	1.3	39.6	121	1.2
	36	0.7	47.5	124	1.3	49.6	203	2.1
brine - tap water	32	0.7	44.3	122	1.3	46.6	162	1.7
	16	0.7	41.2	115	1.2	42.4	144	1.5

the overall plant capacity as the sum of power capacities of the three single RED units.

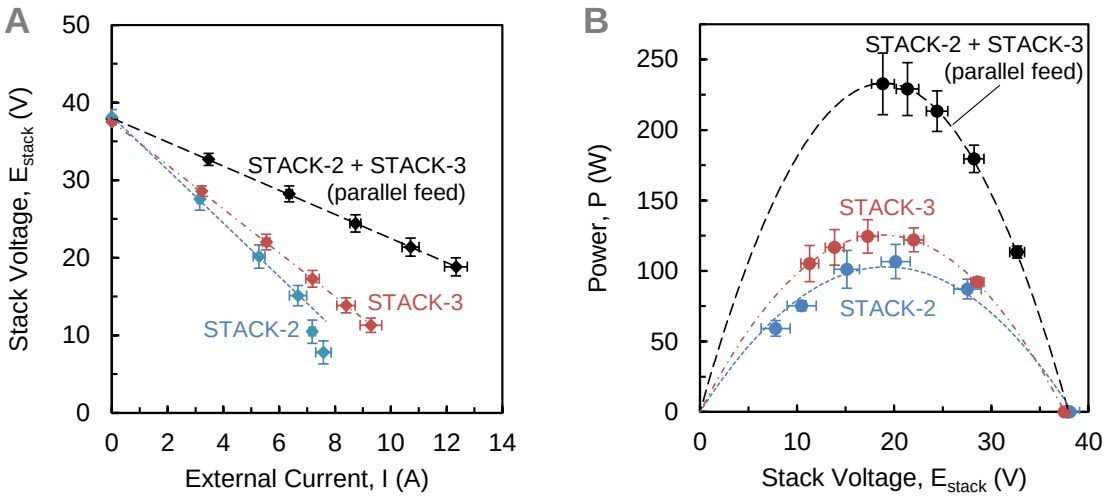

Figure 8: Power measurements with two large prototypes (44x44 cm^2, 500 cell pairs) using brine and brackish water. All measurements were performed operating the stacks in a parallel arrangement for feed solutions, and electrically connected in parallel. Brine conditions: conductivity 210±5 mS/cm, T = 28°C, flow rate 26 l/min. Brackish water conditions: conductivity 3.4 mS/cm, T = 25°C, flow rate 38 l/min. A) Polarization curve. B) Power curve.

Tab. 5 shows an overview of the measurements carried out operating STACK-2 and STACK-3 in parallel.

3.3. Pumping losses and net power output

In order to have a real measure of the net power production, measured pressure drops in the two large stacks were used to calculate the pumping losses within the pilot plant. As shown in Fig. 9, larger pressure drops were found for the HIGH compartment, though it was fed with lower flow rates. This was expected due to the effect of higher viscosity of the brine, which significantly affects

Table 5: Summary of the main results achieved operating STACK-2 and STACK-3 in parallel.

Feed solutions	LOW flow rate (l/min)	LOW conductivity (mS/cm)	OCV (V)	P (W)	Pd (W/m^2)
brine/brackish water	38	3.4	37.9	233	1.2
	32	3.4	35.3	184	0.9
brine - tap water	38	0.7	41.2	266	1.4

friction phenomena inside the spacer-filled channels [36]. On the other hand, only small differences in measured pressure drops can be observed when using natural and artificial solutions.

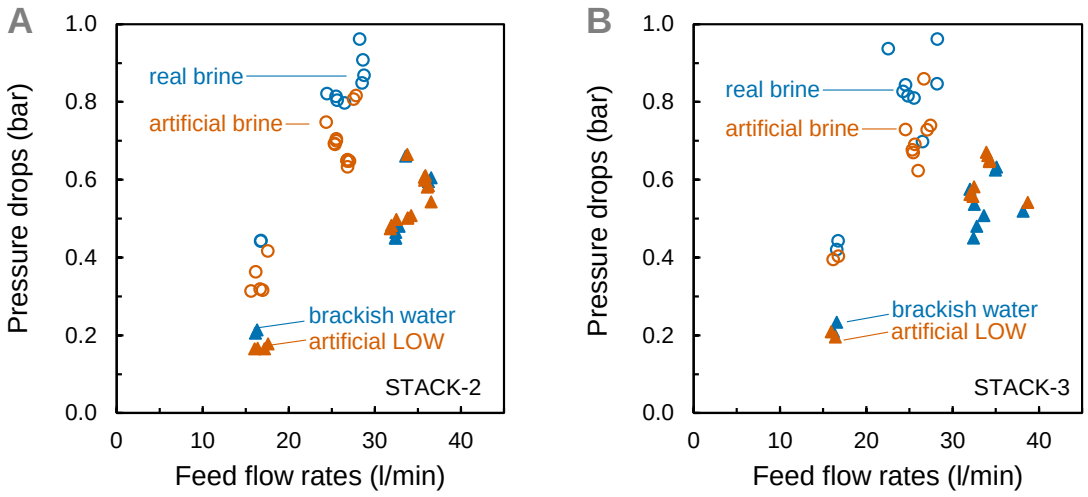

Figure 9: Pressure drops measured in the HIGH and LOW channels of two large RED units, as a function of the feed flow rate. A) Stack-2; B) Stack-3.

From pressure drops and feed flow rates, also the pumping power and net power output were calculated. The values for this latter are reported in Fig. 10. In all cases, a positive net power output was obtained, with larger values between 100 and 250 W for the STACK-3 operated with artificial solutions and lower values for the STACK-2. Using the natural feed streams, the net power output decreases to values between 0 and 100W, with lower values reached again by STACK-2.

3.4. Overall plant capacity and performance

An effective comparison of the three RED units tested in the pilot plant can be given in terms of power density. Fig. 11.A shows how the scale-up of the units from 125 to 500 cell pairs does not lead to a reduction in power density, at the contrary an increase was observed from STACK -1 to STACK-3. Worse performances were measured in STACK-2, likely related to an improvement in the stack-making process for STACK-3, highlighting the importance of working on stack manufacturing and optimisation aspects.

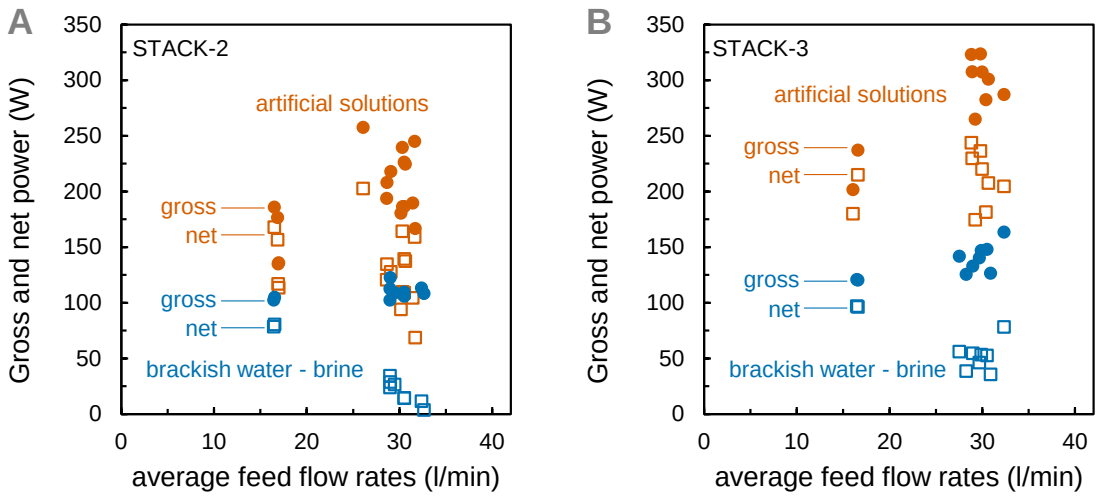

Figure 10: Gross and net power output measured for the two large RED units, fed with artificial and real solutions, as a function of the average (HIGH-LOW) feed flow rate. A) STACK-2. B) STACK-3.

Concerning the overall capacity of the demonstration plant, Fig. 11.B indicates that using artificial solutions, the REAPower pilot plant can reach a power output of almost 700 W, not far from the 1 kW target identified during the design and theoretical analysis of the system [35]. This is especially true considering that theoretical expectations were based on the use of 3 RED units with a 44x44 cm^2 membrane area and 500 cell pairs, while the real plant has two of such units and a smaller third one.

The plant performance drops down when using real brine and brackish water, leading to an overall power capacity around 330 W, thus halved with respect to the one achieved with the artificial NaCl solutions.

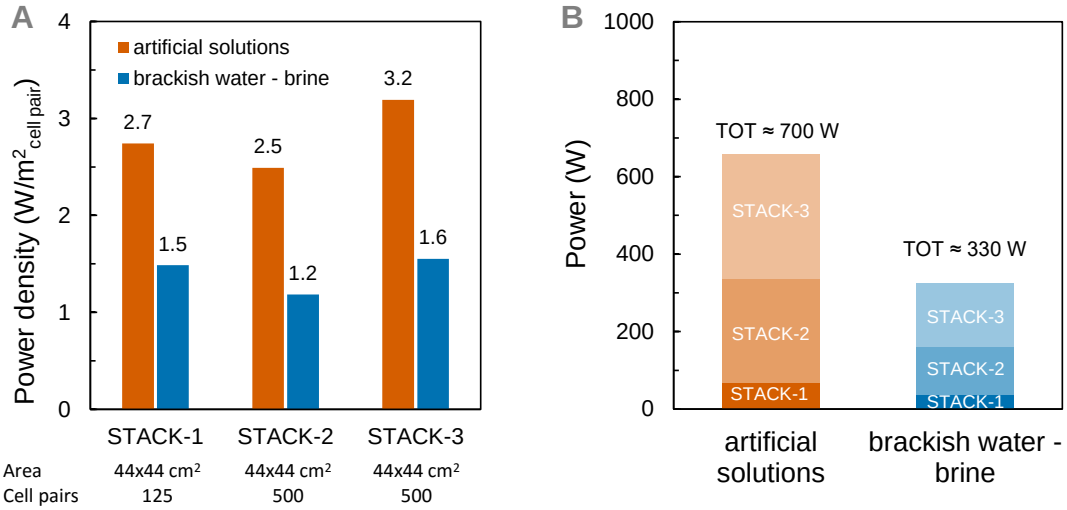

Figure 11: A) Performance comparison for the three RED units tested, expressed in terms of power density (W/m^2 of cell pair). B) Overall plant capacity of the pilot plant. Tests performed using real brackish water (3.4 mS/cm) and brine (190-215 mS/cm), or using artificial (NaCl) solutions with same conductivity as the natural feeds.

4. Conclusions and outlook

An overview of design, commissioning and operational activities of the first RED pilot plant operated with brines and saline waters is presented. The plant, final goal of the EU-funded REAPower project, has reached its final configuration with the installation of three RED prototype units, with an overall ion exchange membrane area over 400 m^2. Testing with artificial and real saline solutions from natural saltworks allowed to characterise the behaviour and the performance of the pilot plant, highlighting strengths and weaknesses of this emerging technologies, in view of the future scale-up possibilities. The system scale-up from 125 cell pairs of the first unit to the 500 cell pairs of the second and third units, did not lead to any reduction of specific performance indicators (e.g. power density). Gross power outputs above 300 W were obtained for STACK-3 operated with artificial solutions, while a drop of ∼50% was observed when real saline solutions were used. This decrease is likely due to the presence of non-NaCl ions highly abundant in the brine, which dramatically affect the stack OCV and resistance. Net power outputs up to 250 W were measured with artificial solutions, reduced to 100 W when using real feed waters.

With an overall plant capacity of almost 700 W using artificial NaCl solutions, and 330 W with real brine and brackish water, the REAPower pilot plant can be considered as the largest application of reverse electrodialysis technology so far reported in the literature, giving a truly demonstration of the process scale-up feasibility. Aside from demonstrating the feasibility of energy production from natural salinity gradients, these results highlight the potential of RED technology with highly concentrated brines for different applications: from the newly proposed RED heat engine [6, 44], to the development of SGP-based energy storage systems, by ED/RED coupling [45, 46].

Future technology developments will focus on a detailed engineering improvement and optimisation of materials and stack manufacturing, including new formulations for IEMs, geometrical optimisation of stack design, possibly towards the use of spacer-less channels. In this regard, profiled membranes have shown already promising results in laboratory studies [29], and recent modelling predictions have indicated how the process performance can be increased significantly by optimised profile design [47, 48].

Acknowledgments

This work has been performed within the REAPower (Reverse Electrodialysis Alternative Power production) project, funded by the EU-FP7 programme (Project Number: 256736). Fujifilm and REDstack are acknowledged for providing membranes and RED units, respectively, along with precious suggestions. The authors are grateful to Claudio Scalici, Davide Vaccari, Carmelo Cirino, Maurizio Bevacqua, and Luigi Gurreri for their help during the construction and testing of the pilot plant.

References

[1] G. Z. Ramon, B. J. Feinberg, E. Hoek, Membrane-based production of salinity-gradient power, Energy & Environmental Science 4 (2011) 4423–4434.

[2] B. E. Logan, M. Elimelech, Membrane-based processes for sustainable power generation using water, Nature 488 (2012) 313–319.

[3] F. Helfer, C. Lemckert, The power of salinity gradients: An Australian example, Renewable and Sustainable Energy Reviews 50 (2015) 1–16.

[4] A. Osorio, S. Ortega, S. Arango-Aramburo, Assessment of the marine power potential in Colombia, Renewable and Sustainable Energy Reviews 53 (2016) 966–977.

[5] J. W. Post, J. Veerman, H. V. M. Hamelers, G. J. W. Euverink, S. J. Metz, K. Nymeijer, C. J. N. Buisman, Salinity-gradient power: Evaluation of pressure-retarded osmosis and reverse electrodialysis, Journal of Membrane Science 288 (2007) 218–230.

[6] A. Tamburini, A. Cipollina, M. Papapetrou, A. Piacentino, G. Micale, Salinity gradient engines, in: Sustainable Energy from Salinity Gradients, Woodhead Publishing Elsevier, 2016.

[7] S. Loeb, Method and apparatus for generating power utilizing reverse electrodialysis (1979).

[8] R. E. Pattle, Production of Electric Power by mixing Fresh and Salt Water in the Hydroelectric Pile, Nature 174 (1954) 660.

[9] F. La Mantia, D. Brogioli, M. Pasta, Capacitive mixing and mixing entropy battery in: Sustainable Energy from Salinity Gradients, Woodhead Publishing Elsevier, 2016.

[10] D. Brogioli, Extracting renewable energy from a salinity difference using a capacitor, Physical Review Letters 103 (2009) 058501(4).

[11] B. B. Sales, M. Saakes, J. W. Post, C. J. N. Buisman, P. M. Biesheuvel, H. V. M. Hamelers, Direct power production from a water salinity difference in a membrane-modified supercapacitor flow cell, Environmental Science and Technology 44 (2010) 5661–5665.

[12] X. Zhu, W. Yang, M. C. Hatzell, B. E. Logan, Energy recovery from solutions with different salinities based on swelling and shrinking of hydrogels., Environmental Science and Technology 48 (2014) 7157–63.

[13] www.redstack.nl/blue-energy.

[14] M. Tedesco, C. Scalici, D. Vaccari, A. Cipollina, A. Tamburini, G. Micale, Performance of the first Reverse Electrodialysis pilot plant for power production from saline waters and concentrated brines, Journal of Membrane Science 500 (2016) 33–45.

[15] R. E. Lacey, Energy by reverse electrodialysis, Ocean Engineering 7 (1980) 1–47.

[16] E. Güler, R. Elizen, M. Saakes, K. Nijmeijer, Micro-structured membranes for electricity generation by reverse electrodialysis, Journal of Membrane Science 458 (2014) 136–148.

[17] J. Liu, G. M. Geise, X. Luo, H. Hou, F. Zhang, Y. Feng, M. A. Hickner, B. E. Logan, Patterned ion exchange membranes for improved power production in microbial reverse-electrodialysis cells, Journal of Power Sources 271 (2014) 437–443.

[18] E. Güler, W. van Baak, M. Saakes, K. Nijmeijer, Monovalent-ion-selective membranes for reverse electrodialysis, Journal of Membrane Science 455 (2014) 254–270.

[19] M. Tedesco, H. V. M. Hamelers, P. M. Biesheuvel, Nernst-Planck transport theory for (reverse) electrodialysis: I. Effect of co-ion transport through the membranes, Journal of Membrane Science 510 (2016) 370–381.

[20] P. Długołecki, J. Dabrowska, K. Nijmeijer, M. Wessling, Ion conductive spacers for increased power generation in reverse electrodialysis, Journal of Membrane Science 347 (2010) 101–107.

[21] L. Gurreri, A. Tamburini, A. Cipollina, G. Micale, M. Ciofalo, Flow and mass transfer in spacer-filled channels for reverse electrodialysis: a CFD parametrical study, Journal of Membrane Science 497 (2016) 300–317.

[22] A. Daniilidis, D. A. Vermaas, R. Herber, K. Nijmeijer, Experimentally obtainable energy from mixing river water, seawater or brines with reverse electrodialysis, Renewable Energy 64 (2014) 123–131.

[23] M. Tedesco, E. Brauns, A. Cipollina, G. Micale, P. Modica, G. Russo, J. Helsen, Reverse Electrodialysis with saline waters and concentrated brines: a laboratory investigation towards technology scale-up, Journal of Membrane Science 492 (2015) 9–20.

[24] G. Geise, A. Curtis, M. C. Hatzell, M. A. Hickner, B. E. Logan, Salt concentration differences alter membrane resistance in reverse electrodialysis stacks, Environmental science & Technology Letters 1 (2014) 36–39.

[25] R. A. Tufa, E. Curcio, W. Van Baak, J. Veerman, S. Grasman, E. Fontananova, G. Di Profio, Potential of brackish water and brine for energy generation by salinity gradient power-reverse electrodialysis (SGP-RE), RSC Advances 4 (2014) 42617–42623.

[26] X. Zhu, W. He, B. E. Logan, Reducing pumping energy by using different flow rates of high and low concentration solutions in reverse electrodialysis cells, Journal of Membrane Science 486 (2015) 215–221.

[27] P. Długołęcki, P. Ogonowski, S. J. Metz, M. Saakes, K. Nijmeijer, M. Wessling, On the resistances of membrane, diffusion boundary layer and double layer in ion exchange membrane transport, Journal of Membrane Science 349 (2010) 369–379.

[28] E. Brauns, Salinity gradient power by reverse electrodialysis: effect of model parameters on electrical power output, Desalination 237 (2009) 378–391.

[29] D. A. Vermaas, M. Saakes, K. Nijmeijer, Power generation using profiled membranes in reverse electrodialysis, Journal of Membrane Science 385–386 (2011) 234–242.

[30] J. Veerman, M. Saakes, S. J. Metz, G. J. Harmsen, Reverse electrodialysis: Performance of a stack with 50 cells on the mixing of sea and river water, Journal of Membrane Science 327 (2009) 136–144.

[31] A. M. Weiner, R. K. McGovern, J. H. Lienhard V, Increasing the power density and reducing the levelized cost of electricity of a reverse electrodialysis stack through blending, Desalination 369 (2015) 140–148.

[32] A. P. Straub, A. Deshmukh, M. Elimelech, Pressure-retarded osmosis for power generation from salinity gradients: is it viable?, Energy & Environmental Science 9 (2016) 31–48.

[33] www.reapower.eu.

[34] M. Tedesco, A. Cipollina, A. Tamburini, I. D. L. Bogle, G. Micale, A simulation tool for analysis and design of reverse electrodialysis using concentrated brines, Chemical Engineering Research and Design 93 (2015) 441–456.

[35] M. Tedesco, P. Mazzola, A. Tamburini, G. Micale, I. D. L. Bogle, M. Papapetrou, A. Cipollina, Analysis and simulation of scale-up potentials in reverse electrodialysis, Desalination and Water Treatment 55 (2015) 3391–3403.

[36] L. Gurreri, A. Tamburini, A. Cipollina, G. Micale, M. Ciofalo, CFD prediction of concentration polarization phenomena in spacer-filled channels for reverse electrodialysis, Journal of Membrane Science 468 (2014) 133–148.

[37] M. Tedesco, A. Cipollina, A. Tamburini, G. Micale, J. Helsen, M. Papapetrou, REAPower: use of desalination brine for power production through reverse electrodialysis, Desalination and Water Treatment 53 (2015) 3161–3169.

[38] A. H. Avci, P. Sarkar, R. A. Tufa, D. Messana, P. Argurio, E. Fontananova, G. Di Profio, E. Curcio, Effect of Mg^{2+} ions on energy generation by Reverse Electrodialysis, Journal of Membrane Science 520 (2016) 499–506.

[39] J. W. Post, H. V. M. Hamelers, C. J. N. Buisman, Influence of multivalent ions on power production from mixing salt and fresh water with a reverse electrodialysis system, Journal of Membrane Science 330 (2009) 65–72.

[40] D. A. Vermaas, J. Veerman, M. Saakes, K. Nijmeijer, Influence of multivalent ions on renewable energy generation in reverse electrodialysis, Energy & Environmental Science 7 (2014) 1434–1445.

[41] A. Cipollina, A. Misseri, G. Staiti, A. Galia, G. Micale, O. Scialdone, Integrated production of fresh water, sea salt and magnesium from sea water, Desalination and Water Treatment 49 (2012) 390–403.

[42] A. Cipollina, M. Bevacqua, P. Dolcimascolo, A. Tamburini, A. Brucato, H. Glade, L. Buether, G. Micale, Reactive crystallisation process for magnesium recovery from concentrated brines, Desalination and Water Treatment 55 (2015) 2377–2388.

[43] O. Scialdone, A. Albanese, A. D. Angelo, A. Galia, C. Guarisco, Investigation of electrode material - Redox couple systems for reverse electrodialysis processes. Part II: Experiments in a stack with 1050 cell pairs, Journal of Electroanalytical Chemistry 704 (2013) 1–9.

[44] www.red-heat-to-power.eu.

[45] R. S. Kingsbury, K. Chu, O. Coronell, Energy storage by reversible electrodialysis: The concentration battery, Journal of Membrane Science 495 (2015) 502–516.

[46] J. W. van Egmond, M. Saakes, S. Porada, T. Meuwissen, C. J. N. Buisman, H. V. M. Hamelers, The concentration gradient flow battery as electricity storage system: Technology potential and energy dissipation, Journal of Power Sources 325 (2016) 129–139.

[47] S. Pawlowski, V. Geraldes, J. G. Crespo, S. Velizarov, Computational fluid dynamics (CFD) assisted analysis of profiled membranes performance in reverse electrodialysis, Journal of Membrane Science 502 (2016) 179–190.

[48] L. Gurreri, M. Ciofalo, A. Cipollina, A. Tamburini, W. van Baak, G. Micale, CFD modelling of profiled-membrane channels for Reverse Electrodialysis, Desalination and Water Treatment 55 (2015) 3404–3423.